



**HAL**  
open science

## **Nigrostriatal dopamine depletion promoted an increase in inhibitory markers (parvalbumin, GAD67, VGAT) and cold allodynia**

Mennatallah Elshennawy, Omar Ouachikh, S Adel Saad, Y Ramadan, Franck Durif, Aziz Hafidi

### ► To cite this version:

Mennatallah Elshennawy, Omar Ouachikh, S Adel Saad, Y Ramadan, Franck Durif, et al.. Nigrostriatal dopamine depletion promoted an increase in inhibitory markers (parvalbumin, GAD67, VGAT) and cold allodynia. *Neuroscience Letters*, 2021, 762, pp.136135. 10.1016/j.neulet.2021.136135 . hal-03584003

**HAL Id: hal-03584003**

**<https://uca.hal.science/hal-03584003v1>**

Submitted on 22 Aug 2023

**HAL** is a multi-disciplinary open access archive for the deposit and dissemination of scientific research documents, whether they are published or not. The documents may come from teaching and research institutions in France or abroad, or from public or private research centers.

L'archive ouverte pluridisciplinaire **HAL**, est destinée au dépôt et à la diffusion de documents scientifiques de niveau recherche, publiés ou non, émanant des établissements d'enseignement et de recherche français ou étrangers, des laboratoires publics ou privés.



Distributed under a Creative Commons Attribution - NonCommercial 4.0 International License

**Nigrostriatal dopamine depletion promoted an increase in inhibitory markers (parvalbumin, GAD67, VGAT) and cold allodynia.**

Mennatallah ELSHENAWY 1,2, Omar OUACHIKH 2, Shereen Adel SAAD 1, Yasmin RAMADAN 1, Franck DURIF 2 and Aziz HAFIDI 2

Affiliations:

1: Anatomy and Embryology Department, Faculty of Medicine, Ain Shams University, Cairo, Egypt

2: Université Clermont Auvergne, CHU, CNRS, Clermont Auvergne INP, Institut Pascal, 63000 Clermont-Ferrand, France.

**Corresponding author:** aziz.hafidi@uca.fr

**Key words:** Parkinson's disease, allodynia, hyperalgesia, cold

**Statistics:** Title: 121 characters including spaces, Text: 4991 words, 8 Figures, 36 References.

**Running Title:** Inhibitory markers' changes in 6-OHDA lesioned rat

**Acknowledgements:** The Missions Sector of Ministry of Higher Education and Scientific Research in Egypt; Ain Shams University, Egypt and Clermont Auvergne University, France funded this study, and all authors declare that there is no conflict of interest.

**Author contributions:** All authors contributed substantially to this study: conception and design of the study (M.E, O.O., A.H.); acquisition and interpretation of data (M.E., O.O, A.H.); drafting of the article (F.D., S.A.S., Y.R.), revising the article critically for important intellectual content (M.E., O.O., A.H.); and final approval of the version to be submitted (M.E., O.O., A.H., F.D., S.A.S., Y.R.).

**Declarations of interest: None**

**Funding:** The Missions Sector of Ministry of Higher Education and Scientific Research in Egypt; Ain Shams University, Egypt and Clermont Auvergne University, France funded this study, and all authors declare that there is no conflict of interest.

E-mail addresses for all authors: [menna.faisal@med.asu.edu.eg](mailto:menna.faisal@med.asu.edu.eg), [omar.ouachikh@uca.fr](mailto:omar.ouachikh@uca.fr), [drshereen\\_youssef@med.asu.edu.eg](mailto:drshereen_youssef@med.asu.edu.eg), [ramdan\\_yasmin@med.asu.edu.eg](mailto:ramdan_yasmin@med.asu.edu.eg), [franck.durif@uca.fr](mailto:franck.durif@uca.fr), [aziz.hafidi@uca.fr](mailto:aziz.hafidi@uca.fr)

## **Highlights**

Pain is the major non-motor symptom in Parkinson's disease.

Dopamine depletion induced changes in excitation and inhibition, as revealed by the changes in different inhibitory and excitatory markers at the level of the spinal dorsal horn.

These changes promoted cold allodynia in dopamine-depleted rats.

## **Abstract**

Pain constitutes the major non-motor symptom in Parkinson's disease (PD). Its mechanism is still poorly understood although an increase in excitation or a decrease in inhibition have been reported in preclinical studies. **The aim of this study was to investigate gamma aminobutyric acid (GABA) inhibition in the 6-hydroxydopamine (6-OHDA) PD rat model.** Therefore, the expression of three inhibitory markers parvalbumin, glutamate decarboxylase 67 (GAD67) and vesicular GABA transporter (VGAT) was evaluated, besides cold allodynia, in bilateral 6-OHDA lesioned rat. There was a significant increase in the expression of the three markers labeling within the spinal dorsal horn (SDH) of 6-OHDA lesioned rats. In parallel, there was also an increase of the excitatory marker protein kinase C gamma (PKC $\gamma$ ) protein. PKC $\gamma$  cells have a crucial role in pain chronicity and are regulated by GABAergic influences. Central dopamine depletion induced an increase in excitation as revealed by an increase in cFOS expression upon acetone stimulus and the presence of cold allodynia. In addition, dopamine depletion induced increased expression in inhibitory markers, which may reflect a disinhibition or a decreased inhibition in 6-OHDA lesioned rats.

## Introduction

Parkinson's disease (PD), which is a neurodegenerative pathology occurring due to loss of dopaminergic neurons in the substantia nigra pars compacta (SNc), entails both motor and non-motor symptoms. PD patients complain of motor symptoms such as resting tremor, rigidity, akinesia and postural instability; while non-motor symptoms are usually stated earlier before PD diagnosis [1,2]. The major non-PD symptom is pain, which constitutes around 68- 95% [3]. Symptoms of pain happen commonly in the off phase of treatment [4] and pain was alleviated on treatment using Levodopa [5]. In PD patients and animal models, many studies have confirmed the decrease in chemical, mechanical and thermal pain thresholds [6,7,8,9]. Although basal ganglia have been implicated in pain, nevertheless, the exact mechanisms integrated in pain pathology are not yet fully discovered [5,6]. In addition, the diminution of dopamine (DA) in striatal pathway has enhanced neuropathic pain [10], while injecting DA receptor 2 (D2R) agonist in the striatum has relieved pain [11,12]. Also, when DA was increased by amphetamine instillation into the nucleus accumbens, pain has been lessened [13].

Neuropathic pain (NP) can be either spontaneous or evoked. Either primary malfunction of the peripheral or central nervous systems may cause NP [14]. It can be manifested as allodynia or hyperalgesia [15,16]. The most common cellular mechanism is an imbalance in neurotransmission with an increase in excitation or disinhibition and/or a decrease in inhibition [15]. Therefore, the goal of the present study was to explore gamma aminobutyric acid (GABA) inhibition in the 6-hydroxydopamine (6-OHDA) rat, which is extensively used as a model of PD [8,17]. Also, two inhibitory markers were explored at the level of the spinal dorsal horn (SDH): vesicular GABA transporter (VGAT) and parvalbumin. VGAT is present in both glycinergic and GABAergic terminals [18], while parvalbumin is present in neurons that co-release GABA and Glycine in the SDH [19, 20]. At last, we explored cold allodynia in this model using acetone stimulus.

## **MATERIALS AND METHODS**

### **Animals**

24 adult male Sprague-Dawley rats (Charles River, France) were used in these experiments. The weight of rats was ranging from 280–350g. Three rats/cage were housed in each cage subjected to optimum laboratory environmental conditions (12/12 light/dark cycle, light on at 7:00 am). Free access to water and food pellets was offered. The experiments followed the animal committee ethical guidelines of Clermont Auvergne University (APAFIS#19965-20190325052285).

### **Surgery**

6-OHDA lesion:

After anesthesia using intraperitoneal injections of (Ketamine 60 mg/kg and xylazine 10 mg/kg), rats have undergone stereotaxic surgery using stereotaxic frame (David Kopf Instrument, CA, USA). Medial Forebrain Bundle was injected bilaterally with 6-OHDA (with rate 0.25  $\mu\text{L}/\text{min}$ ) in two deposits (2.25 and 2.85  $\mu\text{L}$ , respectively). Vehicle saline solution (0.02% ascorbic acid) was used to dissolve 6-OHDA (6-hydroxydopamine hydrochloride) neurotoxin which was injected at a concentration of 3  $\mu\text{g}/\mu\text{L}$  (Sigma-Aldrich, France). Injections were performed at the following coordinates: For 2.25  $\mu\text{L}$  deposit; anterior (A)  $-4.0$ ; lateral (L)  $\pm 0.8$ ; ventral (V)  $-8.0$ ; tooth bar at  $+3.4$  and for 2.85  $\mu\text{L}$  deposit: A  $-4.4$ ; L  $\pm 1.2$ ; V  $-7.8$ ; tooth bar at  $-2.4$  [12]. Desipramine hydrochloride (25 mg/kg, i.p., Sigma-Aldrich) was injected to save adrenergic neurons from degeneration 30 minutes before 6-OHDA injection. Vehicle -only- was injected in sham rats using similar coordinates. The syringe used for injection was retracted with a rate 1 mm/minute. Bilateral 6-OHDA Medial Forebrain Bundle lesion results in rats' aphagia and adipsia, therefore, rats' weight was observed daily. They were syringe fed using wet food pellets, milk and water twice daily until they became independent.

### **Study groups**

There are 3 groups included in this study. Sham, 6-OHDA lesioned and 6-OHDA lesioned rats with acute intraperitoneal administration of D2R agonist which is ropinirole hydrochloride. Ropinirole hydrochloride was given for four days starting at day ten after 6-OHDA lesion surgery. The concentration of ropinirole used was 5mg/Kg/ml (Sigma-Aldrich),

(Elshennawy et al., Submitted). The ropinirole treated group is stated as 6-OHDA +D2R agonist group. Tests were done after two weeks of surgery.

### **Immunohistochemistry**

Rats were deeply anesthetized using ketamine (60 mg/kg) and xylazine (10 mg/kg) intraperitoneal. Acetone stimulus was used as cold allodynic stimulus; acetone drop was gently applied onto the plantar surface of hind paw bilaterally (without touch). **Methodology details are modified from (Dieb et al., 2016) [8]:** Frozen coronal sections (40 $\mu$ m) were cut with a microtome. Spinal cord segments used were lumbar ones (L3–L6). Primary antibodies solutions used were: rabbit monoclonal anti-cFOS (1:2000 Cell Signaling, France), rabbit polyclonal anti-VGAT (1:100 Sigma-Aldrich), mouse monoclonal anti-Parvalbumin (1:200 Sigma-Aldrich), rabbit monoclonal anti-GAD1 (1:1000, Cell Signaling), mouse monoclonal anti-PKC $\gamma$  (1: 500, Santa- Cruz, France) and mouse monoclonal anti-TH antibody (1:5000, Sigma-Aldrich) overnight. After multiple washes, sections were incubated with a secondary antibody solution (1:500 for goat anti-mouse 488; goat anti-rabbit 555, Cell Signaling) for 2 hours at room temperature. At the end, sections were washed and mounted onto Thermo Scientific Superfrost Plus slides (Fisher Scientific, UK), and cover slipped with Dako Fluorescence Mounting Medium (Agilent, USA). Primary antibodies were omitted and there were no signals confirming their specificity of the immunostaining. Immuno-stained sections were photographed using a motorized Zeiss Axioplan 2 microscope. Same area of the spinal cord was used to lessen staining variability among different sections for fluorescent signal quantification. Measurement of cFOS positive cell number was taken from the SDH. A square area of equal dimensions (2x2") was applied for all sections. The Parvalbumin positive cells were counted in Laminae II of SDH. Tyrosine hydroxylase (TH) immunolabeled cells were quantified in the whole sections at different slices at the level of Substantia nigra pars compacta (SNc) and Ventral tegmental area (VTA) {Rostro-caudal sections from (-5.16mm to -6.12mm) were analyzed}. cFOS, Parvalbumin and TH cells were quantified using multipoint cursor in ImageJ Software (ImageJ v1.6, National Institutes of Health). Parvalbumin, VGAT, GAD67 and PKC $\gamma$  fluorescence intensities were measured throughout different spinal cord slices. The number of sections used for each group and each antibody was eight. Fluorescence intensity was measured using Image J software. The RGB image was converted to a grayscale 16-bit image, then the image was duplicated. After that, a threshold was assigned to create a binary image where sliders were adjusted to highlight the expression. The assigned pixels range was used to compare between all groups' sections. Image analysis took place and mean

pixels intensity was measured. Cell counting and fluorescence quantification were done by a blind observer.

### **Western Blot:**

Fresh spinal cord tissues (from L3 to the end of spinal cord) were snap frozen and homogenized with lysis buffer (50mM HEPES, pH 7.5, 1% Triton X-100, 10mM EDTA, 150mM NaCl, 10mM Na<sub>4</sub>P<sub>2</sub>O<sub>7</sub>, 0.1M NaF, 2mM vanadate), extraction buffer was added then centrifuged and supernatants were collected. Samples' proteins amount was assessed using BCA Protein Assay Kit (Pierce-Thermo Scientific, France) and equal amount (40µg) was loaded on 4-20% Mini-PROTEAN TGX polyacrylamide gels (BioRad, France) and transferred using wet blotting system (BioRad). After washing blots with TBS-T (10mM Tris-HCl, pH 7.6, 150mM NaCl, 0.01% Tween-20), they were blocked with 5% BSA in TBS-T for 1 hour at room temperature. Then incubated at 4 °C overnight with primary antibodies diluted in 5 % BSA in TBS-T; mouse monoclonal anti-D2DR (1:250, Santa-Cruz) and rabbit polyclonal anti-GAPDH (0.2 µg/ml, Sigma-Aldrich). Membranes were incubated for 1 hour with HRP-conjugated anti-rabbit and anti-mouse IgG secondary antibodies (1:5,000, Pierce-Thermo Scientific) diluted in 5% BSA in TBS-T. Clarity Western ECL Substrate solution (Bio-Rad) was used to visualize the different bands using ChemiDoc XRS (Bio-Rad, USA).

### **Statistical analysis:**

The results are expressed as mean ± SEM. Statistical analysis was performed using one-way ANOVA to compare between the three groups, followed by post-hoc Tukey's multiple comparisons test for parametric data and Kruskal-Wallis test, followed by post-hoc Dunn's multiple comparisons test for non-parametric data. Student's T-test was used when the comparison between two groups only was required for parametric data. Normality tests were done using D'Agostino-Pearson normality test. The level of significance was determined at P value ≤ 0.05. Data were analyzed using GraphPad Prism Software (v.8.0.2).



## Results

### cFOS expression in the spinal dorsal horn upon acetone stimulation (Figure 1)

cFOS labeling expression upon paw acetone stimulus was observed in superficial and deep laminae of the SDH in sham (Fig.1A), 6-OHDA lesioned (Fig.1B) and 6-OHDA +D2R agonist rats (Fig.1C). cFOS-positive cells were quantified in the SDH laminae in the three animal groups. Pain marker, cFOS positive cells number (Fig.1D), was increased significantly ( $P \leq 0.01$ ) in 6-OHDA lesioned group than sham. There was also a significant ( $P \leq 0.05$ ) difference between 6-OHDA +D2R agonist rats and sham. There was no significant difference between 6-OHDA lesioned and 6-OHDA +D2R agonist groups.

### VGAT expression in the spinal dorsal horn (Figure 2)

VGAT labeling was expressed throughout the SDH laminae in sham (Fig.2A), 6-OHDA lesioned (Fig.2B) and 6-OHDA +D2R agonist animals (Fig.2C). VGAT was observed across superficial and deep SDH laminae. Intense VGAT staining was observed in the SDH of 6-OHDA lesioned when compared to sham. While more intense VGAT staining was observed in 6-OHDA +D2R agonist compared to 6-OHDA lesioned and sham rats. VGAT staining fluorescence comparison (Fig.2D) revealed a **highly** significant ( $P \leq 0.001$ ) difference between the 6-OHDA lesioned and sham. Ropinirole has augmented significantly VGAT; a high level of significance ( $P \leq 0.001$ ) was observed between 6-OHDA +D2R agonist and both 6-OHDA lesioned and sham.

### Parvalbumin expression in the spinal dorsal horn (Figure 3)

In the present study, Parvalbumin labeling is localized in SDH superficial laminae cells in the sham (Fig.3A), 6-OHDA lesioned (Fig.3B) and 6-OHDA +D2R agonist rats (Fig.3C). Within the SDH of all groups, Parvalbumin immunolabeling was observed mostly in cells of lamina II and in scattered cells within lamina III. Parvalbumin labeling was measured using both fluorescence quantification (Fig.3D) and the number of positive cells (Fig.3E). 6-OHDA lesioned has an intense significant ( $P \leq 0.001$ ) increase of Parvalbumin expression more than sham regarding both fluorescence quantification and number of positive cells. Ropinirole decreased the Parvalbumin expression significantly ( $P \leq 0.001$ ) in 6-OHDA +D2R agonist rats compared to 6-OHDA lesioned one regarding both fluorescence quantification and number of positive cells too.

#### **VGAT and Parvalbumin co-labeling in the spinal dorsal horn (Figure 4)**

Double labeling using VGAT and parvalbumin antibodies, (Fig.4A-D) show the presence of VGAT in parvalbumin cells (Fig.4C-D). VGAT staining had a broader cell localization (Fig.4A) than the more restricted parvalbumin one (Fig.4B) within the SDH.

#### **GAD67 expression in the spinal dorsal horn (Figure 5)**

GAD67 labeling was expressed throughout the SDH laminae in sham (Fig.5A), 6-OHDA lesioned (Fig.5B) and 6-OHDA +D2R agonist animals (Fig.5C). GAD67 expression was measured using fluorescence quantification (Fig.5D). 6-OHDA lesioned rats showed a significant increase ( $P \leq 0.001$ ) in GAD67 fluorescence intensity more than both sham and 6-OHDA +D2R agonist. Ropinirole intraperitoneal administration led to a significant diminution ( $P \leq 0.001$ ) of GAD67 expression in 6-OHDA +D2R agonist group **compared to** 6-OHDA lesioned one.

#### **D2DR expression in the spinal dorsal horn (Figure 6)**

Western blot bands (Fig.6A) revealed a significant D2DR protein increase in 6-OHDA lesioned group more than both sham ( $P \leq 0.05$ ) and 6-OHDA +D2R agonist ( $P \leq 0.01$ ) groups (Fig.6B).

#### **PKC gamma expression in the spinal dorsal horn (Figure 7)**

PKC $\gamma$  labeling is localized in SDH superficial laminae cells in sham (Fig. 7A), 6-OHDA lesioned (Fig.7B) and 6-OHDA +D2R agonist rats (Fig.7C). PKC $\gamma$  positive cells were observed within SDH mostly in cells of lamina IIi and in scattered cells within lamina III. PKC $\gamma$  expression was measured using fluorescence quantification (Fig.7D). 6-OHDA lesioned rats had significant ( $P \leq 0.001$ ) increase in PKC $\gamma$  fluorescence quantification compared to both sham and 6-OHDA +D2R agonist groups regarding fluorescence intensity. Ropinirole intraperitoneal administration resulted in a significant decrease ( $P \leq 0.001$ ) of PKC $\gamma$  expression in 6-OHDA +D2R agonist rats when compared to 6-OHDA lesioned ones.

#### **TH expression in SNc and VTA (Figure 8)**

TH labeling was expressed in SNc and VTA in both sham (Fig.8A) and 6-OHDA lesioned groups (Fig.8B) to verify the effect of 6-OHDA toxin in the bilateral MFB lesion. TH labeling was seen in cell bodies and processes **of the dopaminergic cells** in the SNc and VTA. A

remarked severe decrease in the TH staining was present in the 6-OHDA lesioned rats in relation to sham validating dopaminergic cells' degeneration. Quantification of TH cells in both SNc and VTA (Fig.8C) showed an enormous significant decrease in cell number between the 6-OHDA lesioned and sham ( $P \leq 0.001$ ).

**Thus, our 6-OHDA lesioned model was validated by the high dopaminergic cells' degeneration in SNc and VTA using TH labeling. Upon applying a cold stimulus, the expression of CFOS (pain) increased in 6-OHDA lesioned when compared to sham. Also, there was an increase in PKC $\gamma$  (chronic pain) and inhibitory markers (VGAT, Parvalbumin and GAD67) in the 6-OHDA lesioned rats when compared to sham. The markers' increase was diminished upon intraperitoneal ropinirole administration, except for the VGAT. D2DR protein is more expressed in the 6-OHDA lesioned when compared to sham.**

## Discussion

The main result of this study shows that bilateral 6-OHDA lesion induced an increase in the expression of inhibitory cell markers parvalbumin, VGAT and GAD67 in the SDH. **These proteins highlighted an increase in excitation at the level of GABA cells. The increase in their expressions is regulated by cell activity [21, 22].** In addition, cold allodynia is demonstrated by the increase in cFOS expression in the SDH upon acetone stimulation of the paw. Moreover, the use of ropinirole, a D2R agonist, reversed the expression of parvalbumin, GAD67, PKC $\gamma$  and cFOS in the SDH. The use of ropinirole has also been demonstrated to alleviate pain sensitivity in this model (Elshennawy et al., Submitted). The present study showed a clear implication of the dopaminergic system in the changes in inhibitory markers in the SDH and the consequent cold pain sensitivity. In parallel, there was an increase in excitation, which is highlighted, by the increase of PKC $\gamma$  protein in the SDH of 6-OHDA lesioned rats as it was also demonstrated in the medullary dorsal horn [7, 8, 23]. PKC $\gamma$  protein plays an important role in pain chronicity [8, 24]. PKC $\gamma$  cells also play an important role in the transfer of non-noxious stimuli to pain processing pathway through polysynaptic pathway [7]. Parvalbumin cells represent gatekeepers of touch-evoked pain after nerve injury and their ablation in naive mice produce neuropathic pain-like mechanical allodynia via disinhibition of PKC $\gamma$  excitatory interneurons [25]. In addition, PKC $\gamma$  cells receive parvalbumin innervation at both medullary [26] and spinal [25] dorsal horns. The present study showed an increase in excitation at both parvalbumin and PKC $\gamma$  cells as highlighted by the increase in the expression of parvalbumin and PKC $\gamma$  proteins respectively in these cell types.

Parvalbumin cells expressed both GABAergic and Glycinergic subtypes [19, 20]. In the medullary dorsal horn, parvalbumin subtypes were shown to be electrically connected through electrical synapses [26]. Parvalbumin cells might exercise their influences on PKC $\gamma$  cells through a disinhibition (through inhibitory cells that are in direct contact with PKC $\gamma$  cells). Therefore, the decrease in the descending pain control, such as in the 6-OHDA conditions, increases excitation in parvalbumin cells hence disinhibiting PKC $\gamma$  cells. Therefore, both parvalbumin and PKC $\gamma$  are highly activated and their respective expressions of parvalbumin and PKC $\gamma$  proteins are increased. Both parvalbumin [22] and PKC $\gamma$  [7,8] proteins are activity-dependent expressed.

A converse correlation exists between the synthesis of GABA and the expression of GAD67 [27]. GAD67 activity declined when GABA levels were elevated. Therefore, the high expression of GAD67 in the dorsal horn of 6-OHDA lesioned rats may reflect a decrease in GABA level. In addition, GAD67 expression is under dopamine control. For example, dopamine depletion or the use of D2R antagonists produced an increase in GAD67 expression [28]. Moreover, levodopa treatment reversed GAD67 mRNA overexpression in 6-OHDA lesioned rats [29, 30]. Although there is no previous report on this at the spinal cord level in the literature to the best of our knowledge, the administration of ropinirole decreased GAD67 expression in the SDH as demonstrated here by immunohistochemistry.

The high increase of VGAT observed in the 6-OHDA-lesioned rat may reflect an increase in excitation at the level of GABA cells within the SDH. Indeed, VGAT expression is activity dependent [31]. The increase in VGAT expression in the SDH did not reflect an increase in inhibition (GABA release); otherwise, the rats would not have had allodynic behavior. A more recent study using unilateral 6-OHDA lesion showed both an increase and a decrease in VGAT in different GABAergic striatal cell subtypes [32]. Ropinirole increased the VGAT labeling expression in the SDH of 6-OHDA lesioned rats. This result is in accordance with a previous report demonstrating an ipsilateral increase of VGAT mRNA in case of L-Dopa administration in unilateral 6-OHDA lesioned rats [32]. It is clear that dopamine agonists increase the expression of VGAT in the SDH; however, the mechanism involved is still to be determined.

cFOS expression significantly increased in the 6-OHDA lesioned SDH upon acetone stimulation and was present in both SDH superficial and deep laminae. Conversely, ropinirole decreased cFOS expression in the SDH although it was still above the sham level (low expression). The present result shows that central dopaminergic regulation is involved in cold sensitization observed in 6-OHDA lesioned rats. SNc modulated pain through the inhibition of nociceptive inputs at spinal cord neurons [33, 34] or ascending projections to cortical areas such as insular or cingulate cortices [34, 35]. Although, to date, there is no evidence in literature of direct projections from the SNc/VTA to the spinal cord, there is some evidence that the SNc/VTA may influence brainstem descending inhibitory pathways [34,36]. The stimulation of SNc inhibited nociceptive input by activation of spinal cord neurons through dopaminergic descending pathways [33, 35]. The high expression of D2R protein in the 6-

OHDA lesioned rats when compared to sham may probably reveal the lack of dopamine secretion at the level of the SDH.

**Conclusion:** The present study demonstrated that central dopamine depletion promoted disinhibition at the SDH level. This change was responsible for the observed cold allodynia in 6-OHDA lesioned rats.

## References:

1. O. Skogar, J. Lokk, Pain management in patients with Parkinson's disease: challenges and solutions, *J. of multidisciplinary healthcare* 9 (2016) 469–479.
2. M.T. Tseng, C.H. Lin, Pain in early-stage Parkinson's disease: Implications from clinical features to pathophysiology mechanisms, *J. of the Formosan Medical Association* 116(8) (2017) 571-581.
3. C. Buhmann, J. Kassubek and W.H. Jost, Management of Pain in Parkinson's Disease, *J. of Parkinson's disease* 10(s1) (2020) S37–S48.
4. A. Fil, R. Cano-de-la-Cuerdab, E. Muñoz-Hellínb, L. Velac, M. Ramiro-Gonzálezd, C. Fernández-de-las-Peñasb, Pain in Parkinson disease: A review of the literature, *Parkinsonism Relat. Disord.* 19(3) (2013) 285-94.
5. M.R. Young Blood, M.M. Ferro, R.P. Munhoz, H.A. Teive, C.H. Camargo, Classification and Characteristics of Pain Associated with Parkinson's Disease, *Parkinson's disease* 2016 (2016) 6067132.
6. E.H. Chudler, Y. Lu, Nociceptive behavioral responses to chemical, thermal and mechanical stimulation after unilateral, intrastriatal administration of 6-hydroxydopamine, *Brain Res.* 1213 (2008) 41–47.
7. W. Dieb, P. Alvarez, A. Hafidi, PKC gamma-positive neurons gate light tactile inputs to pain pathway through pERK1/2 neuronal network in trigeminal neuropathic pain model, *J. of oral & facial pain and headache* 29 (2015) 70-82.
8. W. Dieb, O. Ouachikh, S. Alves, Y. Boucher, F. Durif, A. Hafidi, Nigrostriatal dopaminergic depletion increases static orofacial allodynia, *J. Headache Pain* 17 (2016) 11.
9. Y. Buhidma, K. Rukavina, K.R. Chaudhuri, S. Duty, Potential of animal models for advancing the understanding and treatment of pain in Parkinson's disease, *npj. Parkinsons Dis.* 6 (2020) 1.
10. R. Takeda, T. Ikeda, F. Tsuda, H. Abe, H. Hashiguchi, Y. Ishida, T. Nishimori, Unilateral lesions of mesostriatal dopaminergic pathway alters the withdrawal response of the rat hindpaw to mechanical stimulation, *Neurosci. Res.* 52 (2005) 31–36.
11. J.E. Magnusson, K. Fisher, The involvement of dopamine in nociception: The role of D(1) and D(2) receptors in the dorsolateral striatum, *Brain Res.* 855(2) (2000) 260-6.
12. A. Wawrzczak-Bargieła, B. Ziółkowska, A. Piotrowska, J. Starnowska-Sokol, E. Rojewska, J. Mika, B. Przewlocka, R. Przewlocki, Neuropathic Pain Dysregulates Gene Expression of the Forebrain Opioid and Dopamine Systems, *Neurotox. Res.* 37 (2020) 800–814.

13. H.N. Harris, Y.B. Peng, Evidence and explanation for the involvement of the nucleus accumbens in pain processing, *Neural Regen. Res.* 15(4) (2020) 597-605.
14. F. Viana, Nociceptors: thermal allodynia and thermal pain, *Handb. Clin. Neurol.* 156 (2018) 103-119.
15. J. Sandkühler, Models and mechanisms of hyperalgesia and allodynia, *Physiol. Rev.* 89 (2009) 707–758.
16. T.S. Jensen, N.B. Finnerup, Allodynia and hyperalgesia in neuropathic pain: Clinical manifestations and mechanisms, *The Lancet Neurology* 13 (2014) 924–935.
17. W. Dieb, O. Ouachikh, F. Durif, A. Hafidi, Lesion of the dopaminergic nigrostriatal pathway induces trigeminal dynamic mechanical allodynia, *Brain Behav.* 4(3) (2014) 368–380.
18. A. Dumoulin, P. Rostaing, C. Bedet, S. Levi, M. Isambert, T. Antoine, B. Gasnier, Presence of the vesicular inhibitory amino acid transporter in GABAergic and glycinergic synaptic terminal boutons, *J. of cell science*, 112 (Pt 6) (1999) 811-23.
19. A.J. Todd, A.C. Sullivan, Light microscope study of the coexistence of GABA-like and glycine-like immunoreactivities in the spinal cord of the rat, *J. Comp. Neurol.* 296 (1990) 496–505.
20. I. Laing, A.J. Todd, C.W. Heizmann, H.H. Schmidt, Subpopulations of GABAergic neurons in laminae I-III of rat spinal dorsal horn defined by coexistence with classical transmitters, peptides, nitric oxide synthase or parvalbumin, *Neuroscience* 61 (1994) 123–132.
21. J. Van Liefferinge, A. Massie, J. Portelli, G. Di Giovanni, I. Smolders, Are vesicular neurotransmitter transporters potential treatment targets for temporal lobe epilepsy? *Frontiers in cellular neuroscience* 7 (2013) 139.
22. J.B. Ruden, L.L. Dugan, C. Konradi, Parvalbumin interneuron vulnerability and brain disorders, *Neuropsychopharmacology* 46(2) (2021) 279-287.
23. W. Dieb, A. Hafidi, Astrocytes are involved in trigeminal dynamic mechanical allodynia: potential role of D-serine, *J. Dent. Res.* 92(9) (2013) 808-13.
24. W. Dieb, A. Hafidi, Mechanism of GABA-involvement in posttraumatic trigeminal neuropathic pain: Activation of neuronal circuitry composed by PKC  $\gamma$  interneurons and pERK1/2 expressing neurons, *Eur. J. Pain* 19 (2015) 85–96.
25. H. Petitjean, S.A. Pawlowski, S.L. Fraine, B. Sharif, D. Hamad, T. Fatima, J. Berg, C.M. Brown, L.Y. Jan, A. Ribeiro-da-Silva, J.M. Braz, A.I. Basbaum, R. Sharif-Naeini, Dorsal Horn Parvalbumin Neurons Are Gate-Keepers of Touch-Evoked Pain after Nerve Injury, *Cell Rep.* 13(6) (2015) 1246-1257.



26. O. Ouachikh, A. Hafidi, Y. Boucher, W. Dieb, Electrical Synapses are Involved in Orofacial Neuropathic Pain, *Neuroscience* 382 (2018) 69-79.
27. K. Rimvall, D.L. Martin, Increased intracellular gamma-aminobutyric acid selectively lowers the level of the larger of two glutamate decarboxylase proteins in cultured GABAergic neurons from rat cerebral cortex, *J. Neurochem.* 58(1) (1992) 158-66.
28. J.J. Soghomonian, M.F. Chesselet, Effects of nigrostriatal lesions on the levels of messenger RNAs encoding two isoforms of glutamate decarboxylase in the globus pallidus and entopeduncular nucleus of the rat, *Synapse* 11(2) (1992) 124-33.
29. C. Périer, C. Marin, A. Jimenez, M. Bonastre, E. Tolosa, E.C. Hirsch, Effect of subthalamic nucleus or entopeduncular nucleus lesion on levodopa-induced neurochemical changes within the basal ganglia and on levodopa-induced motor alterations in 6-hydroxydopamine-lesioned rats: STN or EP lesion on levodopa-induced changes, *Journal of Neurochemistry* 86(6) (2003) 1328–1337.
30. J.J. Bacci, P. Salin, L. Kerkerian-Le Goff, Systemic administration of dizocilpine maleate (MK-801) or L-dopa reverses the increases in GAD65 and GAD67 mRNA expression in the globus pallidus in a rat hemiparkinsonian model, *Synapse* 46(4) (2002) 224-234.
31. R. Gutiérrez, Activity-dependent expression of simultaneous glutamatergic and GABAergic neurotransmission from the mossy fibers in vitro, *J. Neurophysiol.* 87(5) (2002) 2562-70.
32. H. Wang, J. Katz, P. Dagostino, J.J. Soghomonian, Unilateral 6-hydroxydopamine lesion of dopamine neurons and subchronic L-DOPA administration in the adult rat alters the expression of the vesicular GABA transporter in different subsets of striatal neurons and in the substantia nigra, pars reticulata, *Neuroscience* 145(2) (2007) 727-37.
33. C.D. Barnes, S.J. Fung, W.L. Adams, Inhibitory effects of substantia nigra on impulse transmission from nociceptors, *Pain* 6 (1979) 207–215.
34. R.M. Beckstead, V.B. Domesick, W.J.H. Nauta, Efferent connections of the substantia nigra and ventral tegmental area in the rat, *Brain Research* 175(2) (1979) 191-217.
35. A. Burkey, E. Carstens, L. Jasmin, Dopamine reuptake inhibition in the rostral agranular insular cortex produces antinociception, *J. Neurosci.* 19 (1999) 4169–4179.
36. G. Halliday, S. Reyes, K. Double, Substantia Nigra, Ventral Tegmental Area, and Retrobulbar Fields, In: *The human nervous system*, ed. 3 (J.K. Mai, G. Paxinos), Academic press, (2012), ch 13, pp. 439-455.

## Figures' legends

**Figure 1:** cFOS protein expression upon acetone stimulus. Figure shows cFOS expression in SDH of sham (A), 6-OHDA lesioned (B) and 6-OHDA +D2R agonist group (C). Graph (D) represents cFOS positive cells within SDH superficial and deep laminae (Kruskal-Wallis test,  $p= 0.0016$ ): 6-OHDA lesioned had more significant number than sham (Dunn's multiple comparisons test,  $p =0.0019$ );  $**p \leq 0.01$ . Also, there was an increase in significance (Dunn's multiple comparisons test,  $p =0.0249$ ) of 6-OHDA +D2R agonist group more than sham;  $*p \leq 0.05$ . Data are means  $\pm$  SEM of 4 animals/group. Scale bar represents 50  $\mu\text{m}$ .

**Figure 2:** The figure shows VGAT immunolabeling in the SDH of sham (A), 6-OHDA lesioned (B) and 6-OHDA +D2R agonist group (C). Graph (D) represents VGAT fluorescence quantification within SDH superficial and deep laminae (one-way ANOVA,  $p <0.0001$ ,  $F(2, 21) =46.35$ ): 6-OHDA lesioned had more significant number than sham (Tukey's multiple comparisons test,  $p =0.0010$ );  $***p \leq 0.001$ . Also, there was an intense increase in significance (Tukey's multiple comparisons test,  $p <0.0001$ ) of 6-OHDA +D2R agonist group more than both sham and 6-OHDA lesioned;  $***p \leq 0.001$ . Data are means  $\pm$  SEM of 4 animals/group. Scale bar represents 50  $\mu\text{m}$ .

**Figure 3:** The figure shows Parvalbumin immunolabeling in sham (A), 6-OHDA lesioned (B) and 6-OHDA +D2R agonist group (C). Graph (D) represents Parvalbumin fluorescence quantification within cells of lamina II and in scattered cells within lamina III (one-way ANOVA,  $p <0.0001$ ,  $F(2, 37) =92.97$ ): 6-OHDA lesioned had more significant intensity than both sham and 6-OHDA +D2R agonist groups (Tukey's multiple comparisons test,  $p <0.0001$ );  $***p \leq 0.001$ . Also, there was an increase in significance of 6-OHDA +D2R agonist group more than sham (Tukey's multiple comparisons test,  $p <0.0001$ );  $***p \leq 0.001$ . Ropinirole administration decreased dramatically the expression of Parvalbumin; where 6-OHDA +D2R agonist group had less fluorescence quantification than 6-OHDA lesioned one ( $***p \leq 0.001$ ). Graph (E) represents Parvalbumin number of cells (one-way ANOVA,  $p <0.0001$ ,  $F(2, 21) =38.39$ ): 6-OHDA lesioned had more significant number than both sham and 6-OHDA +D2R agonist groups (Tukey's multiple comparisons test,  $p <0.0001$ , 0.0002 respectively);  $***p \leq 0.001$ . Also, there was an increase in significance of 6-OHDA +D2R agonist group more than sham (Tukey's multiple comparisons test,  $p =0.0025$ );  $**p \leq 0.01$ . Ropinirole administration decreased the expression of Parvalbumin; where 6-OHDA +D2R

agonist group had less number of cells than 6-OHDA lesioned one (\*\* $p \leq 0.01$ ). Data are means  $\pm$  SEM of 4 animals/group. Scale bar represents 50  $\mu\text{m}$ .

**Figure 4:** Co-labeling of VGAT and parvalbumin antibodies, (Fig.4A-D) reveal the expression of VGAT in parvalbumin cells (Fig.4C-D). VGAT labelling had a wider cell localization (Fig.4A) than the more restricted parvalbumin one (Fig.4B) within the SDH lamina II and in scattered cells within lamina III. Scale bar represents 50 $\mu\text{m}$  for A-C and 20 $\mu\text{m}$  for D.

**Figure 5:** GAD67 protein expression. The figure shows GAD67 expression in SDH of sham (A), 6-OHDA lesioned (B) and 6-OHDA +D2R agonist group (C). Graph (D) represents GAD67 fluorescence quantification within SDH (one-way ANOVA,  $p < 0.0001$ ,  $F(2, 21) = 97.18$ ): 6-OHDA lesioned had increased significance than both sham and 6-OHDA +D2R agonist groups (Tukey's multiple comparisons test,  $p < 0.0001$ ); \*\*\* $P \leq 0.001$ . Data are means  $\pm$  SEM of 4 animals/group. Scale bar represents 50  $\mu\text{m}$ .

**Figure 6:** Figure (A) represents western blot bands of D2R expression of sham, 6-OHDA lesioned and 6-OHDA +D2R agonist group. Graph (B) shows relative intensities of bands of the three groups (one-way ANOVA test,  $p = 0.0021$ ,  $F(2, 9) = 13.17$ ): 6-OHDA lesioned had more significant increase in expression than both sham and 6-OHDA +D2R agonist groups (Tukey's multiple comparisons test,  $p = 0.0154$ ,  $p = 0.0019$  respectively); \* $P \leq 0.05$ , \*\* $P \leq 0.01$ . Data are means  $\pm$  SEM of 4 animals/group, GAPDH was used as the loading control.

**Figure 7:** PKC $\gamma$  protein expression. Figure shows PKC $\gamma$  expression in SDH of sham (A), 6-OHDA lesioned (B) and 6-OHDA +D2R agonist group (C). PKC $\gamma$  positive cells were located within SDH in cells of lamina II and in scattered cells within lamina III. Graph (D) represents PKC $\gamma$  fluorescence quantification (one-way ANOVA,  $p < 0.0001$ ,  $F(2, 21) = 22.43$ ): 6-OHDA lesioned had more significance than both sham and 6-OHDA +D2R agonist groups (Tukey's multiple comparisons test,  $p < 0.0001$ ); \*\*\* $P \leq 0.001$ . Data are means  $\pm$  SEM of 4 animals/group. Scale bar represents 50  $\mu\text{m}$ .

**Figure 8:** TH immunolabeling in sham (A) and 6-OHDA lesioned animals (B) indicates an extreme decrease in the intensity of labeling, in both SNc and VTA in 6-OHDA lesioned animals in comparison to sham ones. Graph (C) shows cell count of TH immunolabeled cells in both SNc and VTA together (student's T-test,  $p < 0.001$ ); \*\*\* $P \leq 0.001$ . Data are means  $\pm$  SEM of 5 animals/group. Scale bar represents 200  $\mu\text{m}$ .

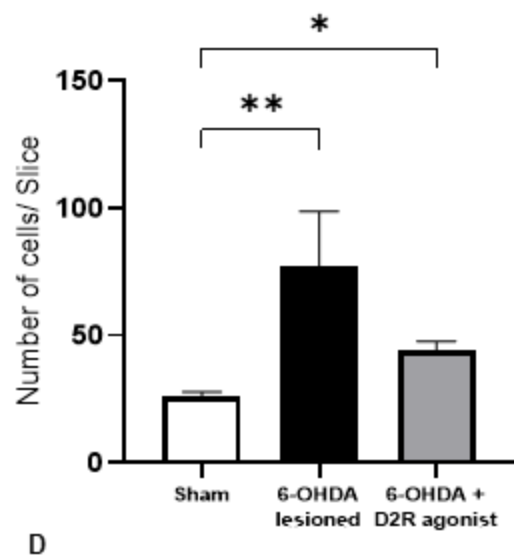
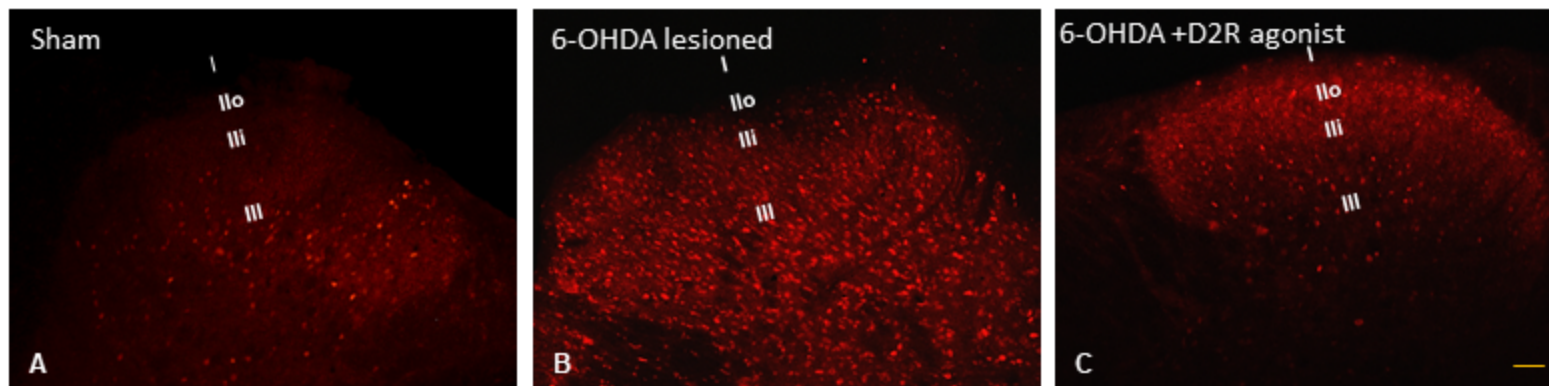


Figure 1

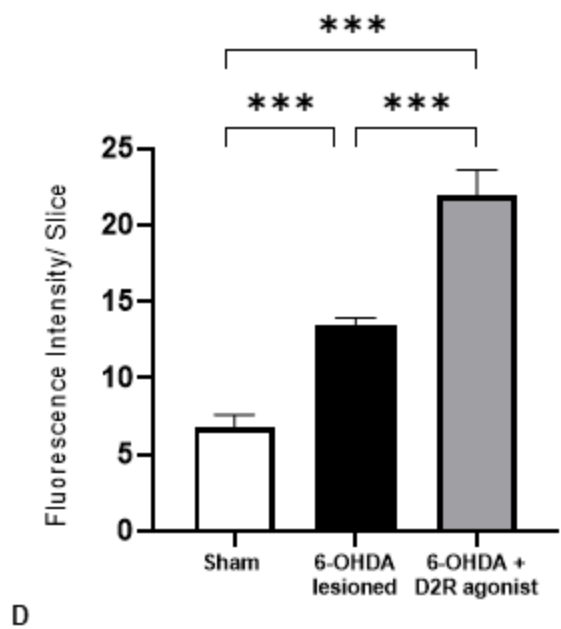
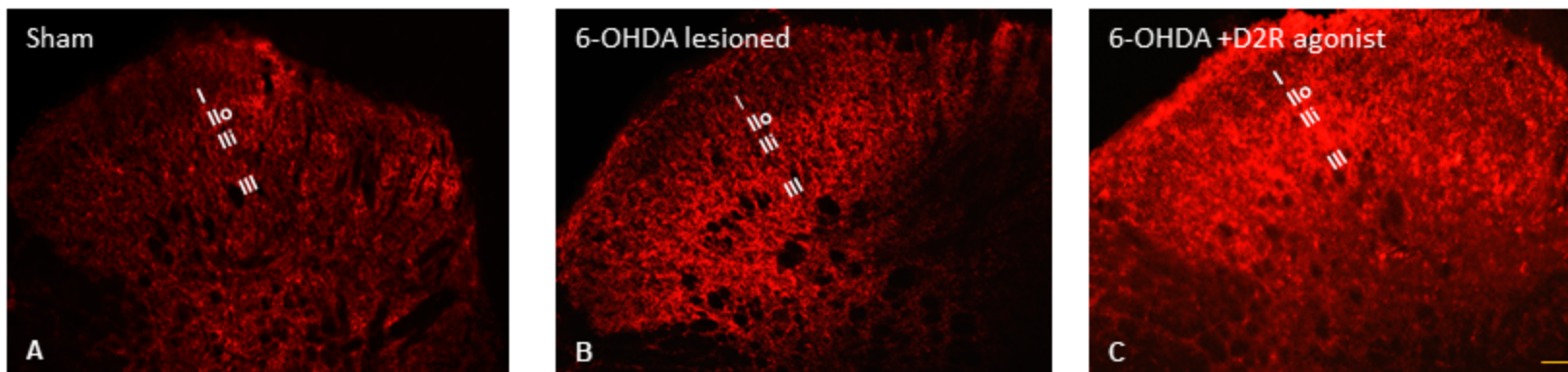
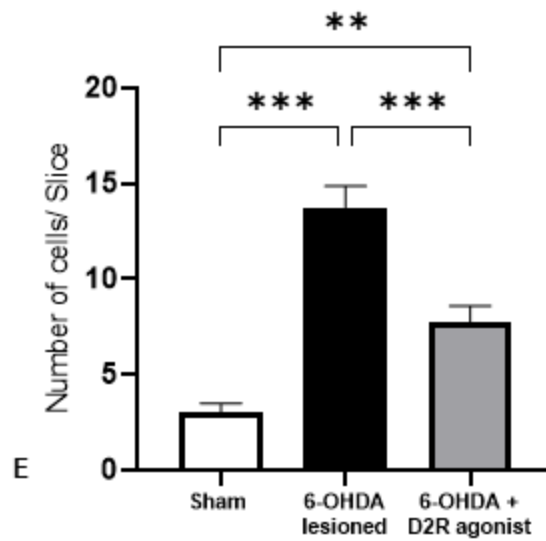
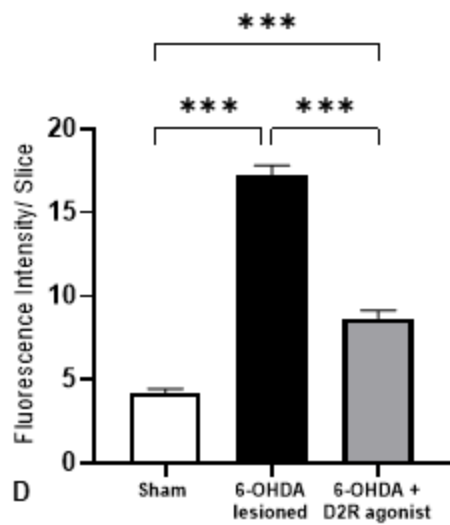
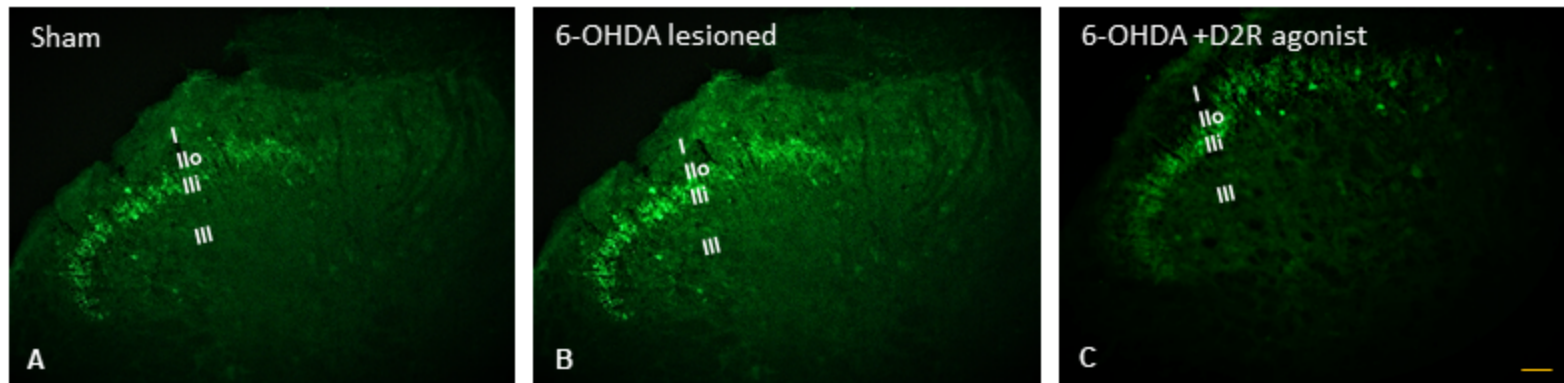
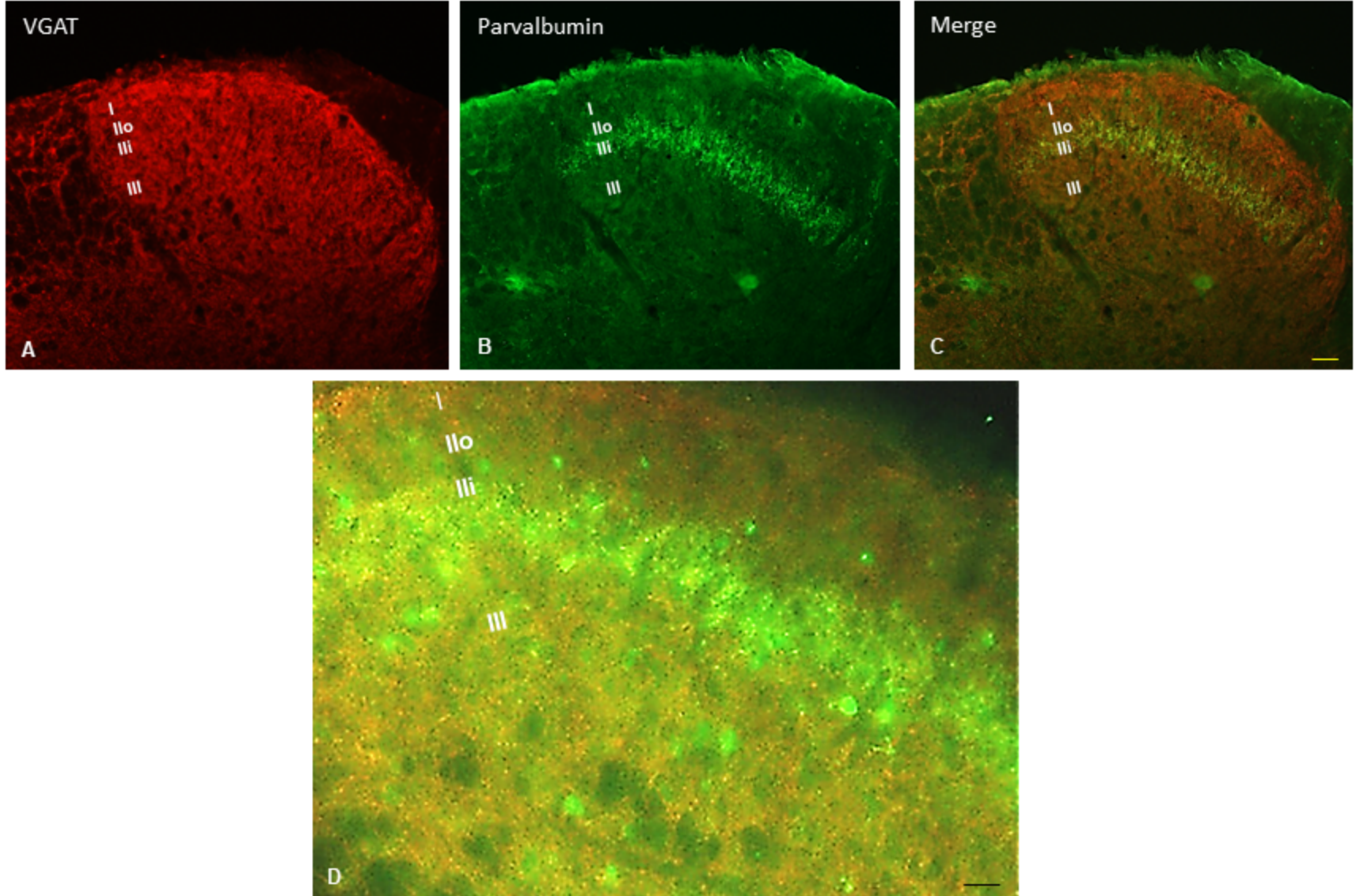


Figure 2



**Figure 3**



**Figure 4**

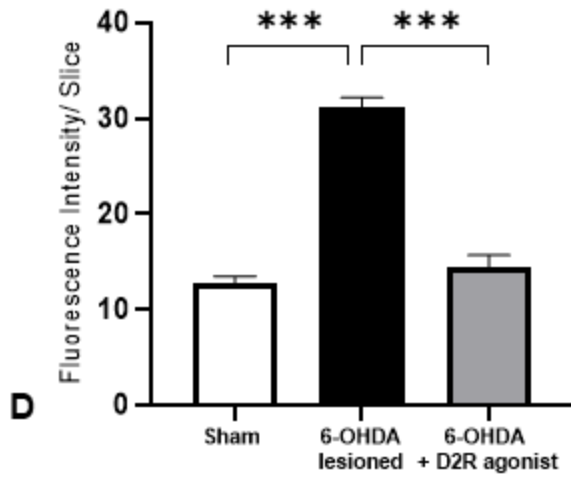
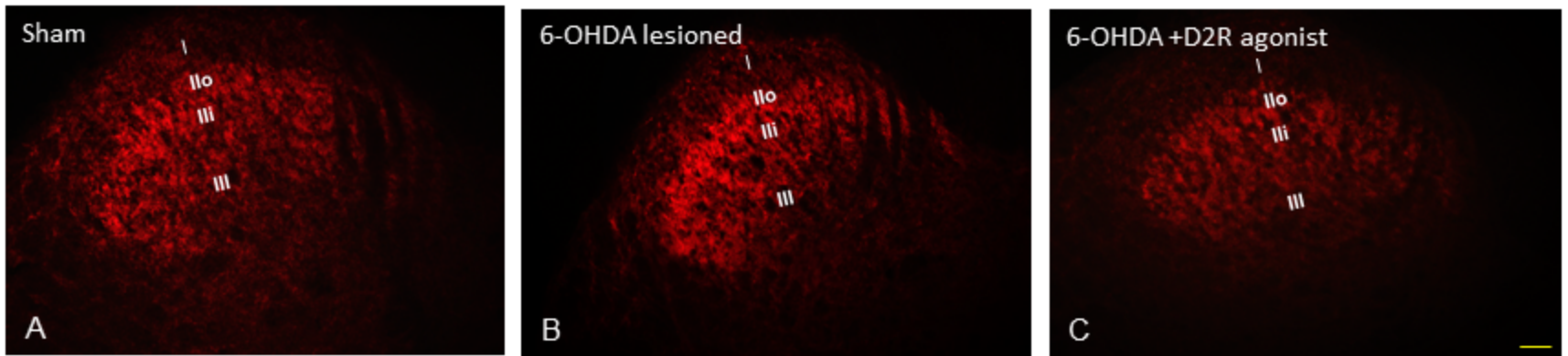
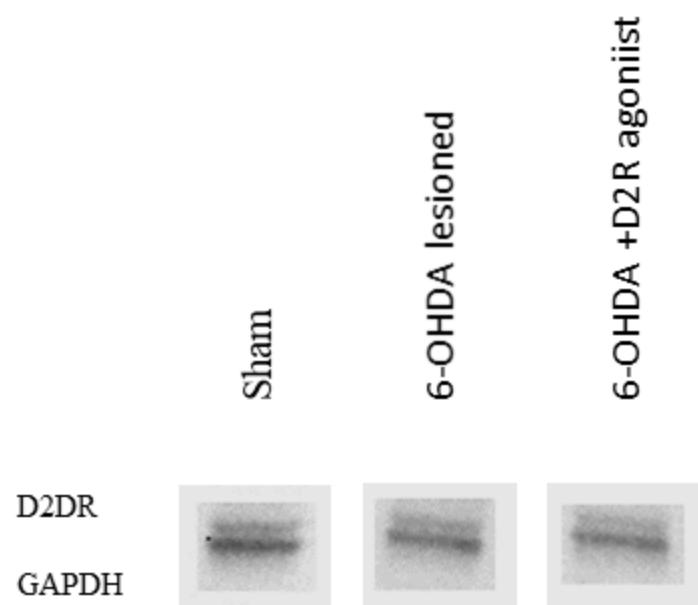
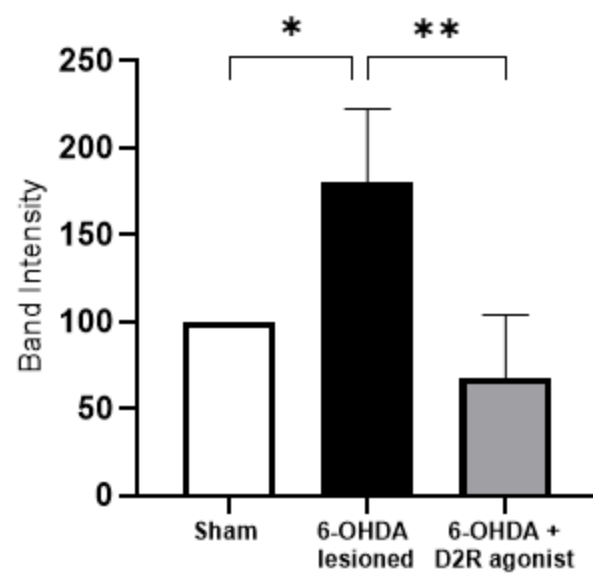


Figure 5



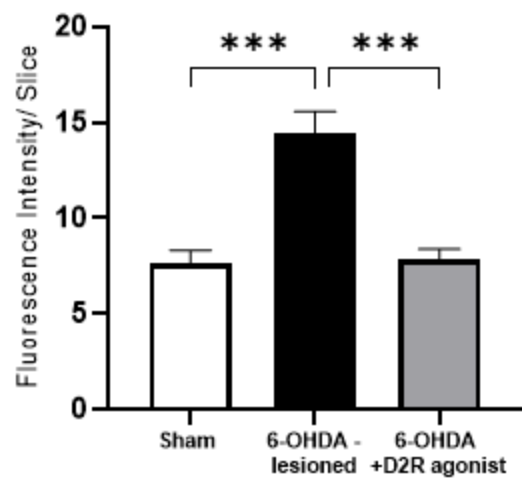
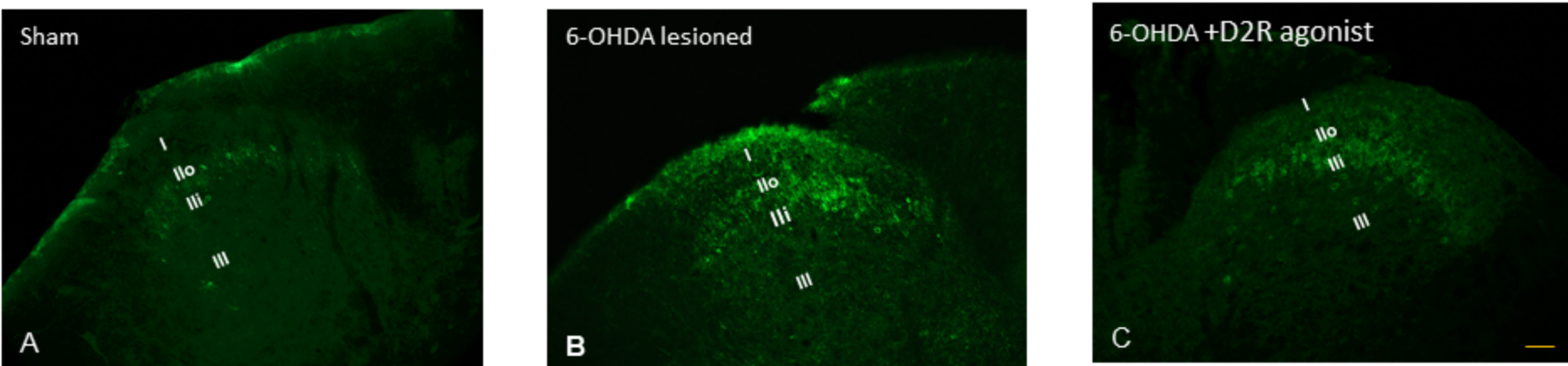


A



B

Figure 6



D

Figure 7

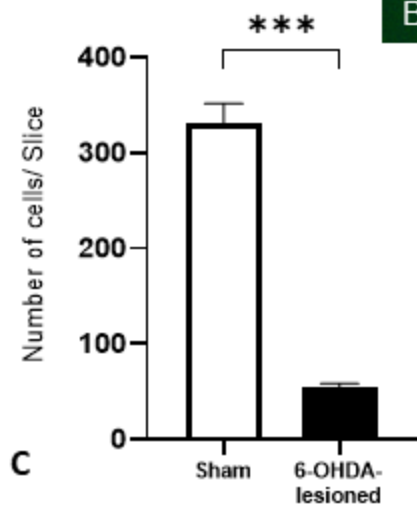
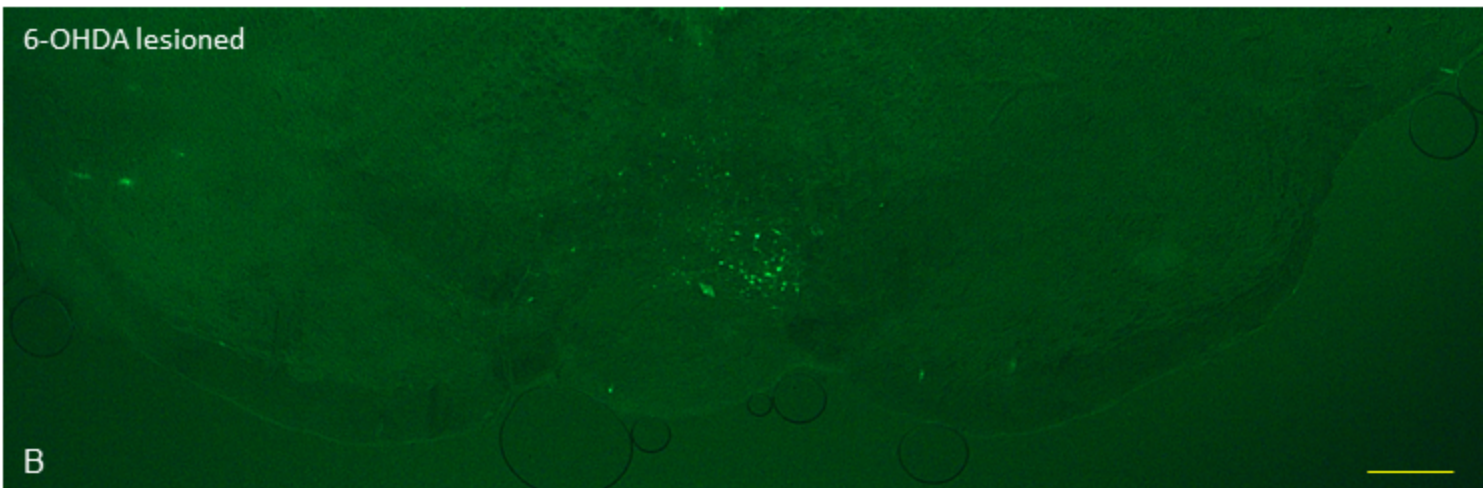
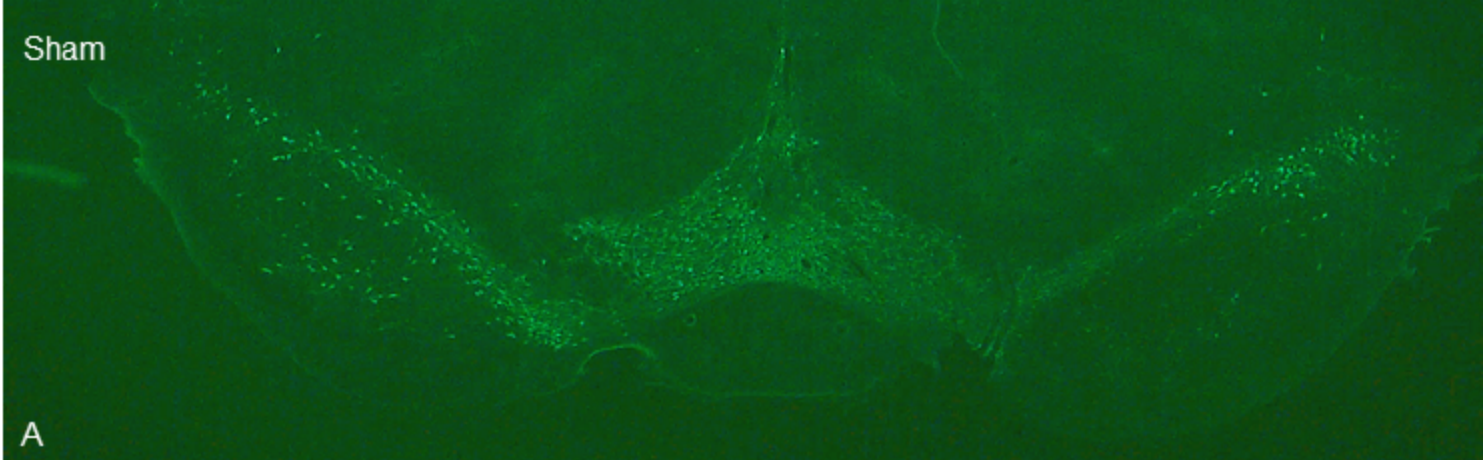


Figure 8